

Engineered heart tissue maturation inhibits cardiomyocyte proliferative response to cryoinjury

Journal of Tissue Engineering
Volume 14: 1–13
© The Author(s) 2023
Article reuse guidelines:
sagepub.com/journals-permissions
DOI: 10.1177/20417314231190147
journals.sagepub.com/home/tej



Giulio Ciucci^{1*}, Karim Rahhali^{1,4}, Giovanni Cimmino²,
Francesco Natale², Paolo Golino², Gianfranco Sinagra³,
Chiara Collesi^{3,4} and Francesco S Loffredo^{1,2*} 

Abstract

The cellular and molecular mechanisms that are responsible for the poor regenerative capacity of the adult heart after myocardial infarction (MI) are still unclear and their understanding is crucial to develop novel regenerative therapies. Considering the lack of reliable in vitro tissue-like models to evaluate the molecular mechanisms of cardiac regeneration, we used cryoinjury on rat Engineered Heart Tissues (rEHTs) as a new model which recapitulates in part the in vivo response after myocardial injury of neonatal and adult heart. When we subjected to cryoinjury immature and mature rEHTs, we observed a significant increase in cardiomyocyte (CM) DNA synthesis when compared to the controls. As expected, the number of mitotic CMs significantly increases in immature rEHTs when compared to mature rEHTs, suggesting that the extent of CM maturation plays a crucial role in their proliferative response after cryoinjury. Moreover, we show that cryoinjury induces a temporary activation of fibroblast response in mature EHTs, similar to the early response after MI, that is however incomplete in immature EHTs. Our results support the hypothesis that the endogenous maturation program in cardiac myocytes plays a major role in determining the proliferative response to injury. Therefore, we propose rEHTs as a robust, novel tool to in vitro investigate critical aspects of cardiac regeneration in a tissue-like asset free from confounding factors in response to injury, such as the immune system response or circulating inflammatory cytokines.

Keywords

Engineered heart tissue, cardiac regeneration, cardiomyocytes, cryoinjury

Date received: 7 March 2023; accepted: 11 July 2023

¹Molecular Cardiology, International Centre for Genetic Engineering and Biotechnology (ICGEB), Trieste, Friuli-Venezia Giulia, Italy

²Department of Translational Medical Sciences, Division of Cardiology, University of Campania “L. Vanvitelli,” Naples, Italy

³Department of Medicine, Surgery and Health Sciences, Azienda Sanitaria-Universitaria Integrata Trieste “ASUITS,” University of Trieste, Trieste, Italy

⁴Molecular Medicine, International Centre for Genetic Engineering and Biotechnology (ICGEB), Trieste, Italy

*These authors contributed equally to this work.

Corresponding authors:

Francesco S Loffredo, Department of Translational Medical Sciences, Division of Cardiology, University of Campania “Luigi Vanvitelli,” Via L. Bianchi, Naples 80131, Italy.

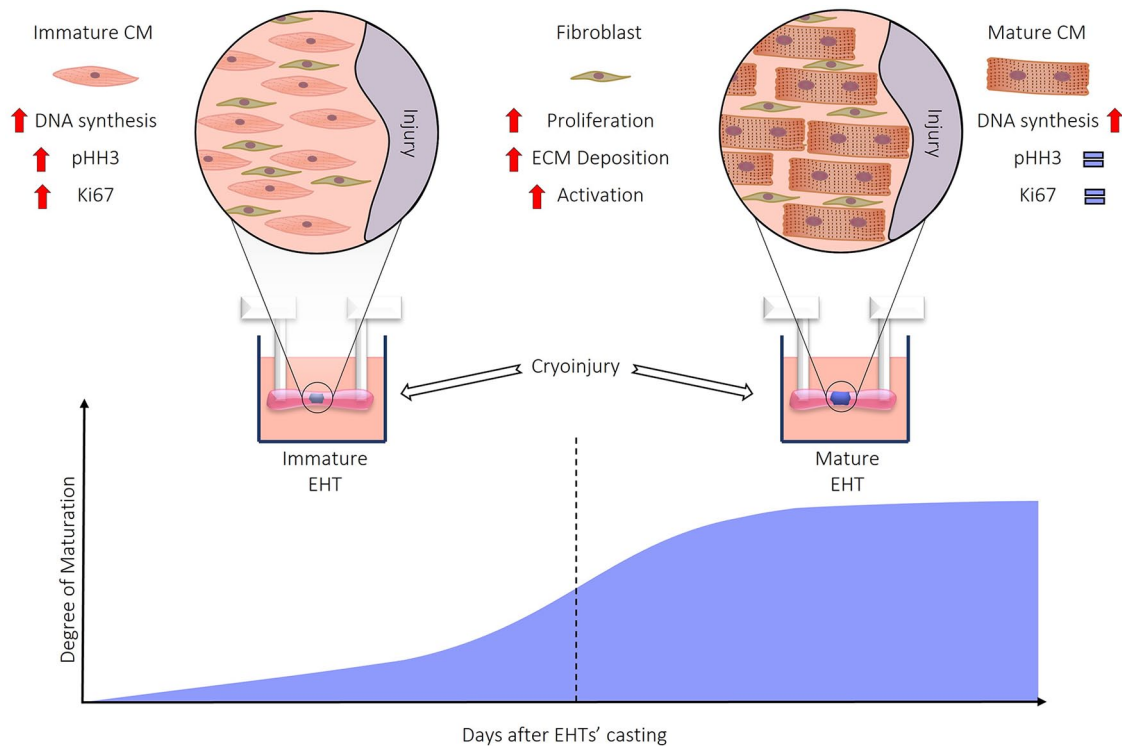
Email: francesco.loffredo@unicampania.it

Giulio Ciucci, Molecular Cardiology, International Centre for Genetic Engineering and Biotechnology (ICGEB), Trieste, Padriciano 99 34012 Friuli-Venezia Giulia, Italy.

Email: ciucci@icgeb.org



Graphical abstract



Introduction

The loss of cardiomyocytes (CMs) after myocardial infarction (MI), replaced by fibrotic tissue, determines different scar sizes, which correlates to prognosis and outcome. As heart diseases are the leading cause of death in the 21st century, understanding the cellular and molecular mechanisms responsible for the poor regenerative capacity of the adult heart is crucial to develop novel regenerative therapies. In rodents, the lack of regenerative response is due to the loss of proliferative capacity of adult CMs, accompanied by an increase in sarcomeric organization and cell size.¹

The lack of reliable *in vitro* tissue-like models to recapitulate cardiac regeneration, in particular as a consequence of myocardial injury,² represents a major limitation in the field. Human Induced Pluripotent Stem Cells (hiPSC) established a reliable protocol to induce CM differentiation providing a robust model to investigate different aspects of human cell biology.³ Unfortunately, the “immature” phenotype remains a thorny problem of the iPSC-derived CMs, limiting the understanding of mechanisms that lie behind the features of adult cardiac cells.⁴ Moving iPSC cultures from the 2D to the 3D topology in EHTs improved CM maturation, obtaining a tridimensional cytological asset that resembles the *in vivo* heart tissue organization.⁵ Nonetheless, *in vitro* human engineered cardiac tissues display an unmatched response to injury compared to adult cardiac tissue.⁶ Rat engineered heart tissues (rEHTs) are made from an unpurified, native heart

cell mix, organized in an *in vivo*-like tridimensional structure,⁷ recapitulating in part the tissue biology of the adult rodent heart, thus representing an exciting candidate to evaluate the effect of myocardial injury in a controlled manner. Indeed, although EHTs model is devoid of the cellular contribution of the immune system and the inflammatory infiltrate, major players in the cellular and molecular response after injury, this may be seen as an advantage when dissecting the peculiar role of CMs. Considering the technical challenge of inducing an infarct-like lesion in an *in vitro* system, we used cryoinjury to deliver a discrete and reproducible lesion in a peculiar and spatially defined area of the rEHTs. As reported previously, *in vivo*, cryoinjury generates a necrotic wound of consistent size and shape that resolves into a scar of uniform size, shape, and molecular organization.⁸ Moreover, the edges of the cryoinjured tissue exhibit classic markers of remodeling found in surviving cardiac tissue at the edge of myocardial infarction.⁹ In this work, using rEHTs as a model, we show that the intrinsic maturation process of CMs regulates the proliferative response of the contractile tissue to cryoinjury, recapitulating in part the *in vivo* biological response to heart damage.¹⁰

Methods

Neonatal rat cardiomyocytes isolation

Hearts from 10 to 15 neonatal Wistar rats (postnatal day 0–3) were minced and subjected to serial DNase/Trypsin

digestion to release single cells. Cell fractions were collected in Fetal Calf Serum (FCS; Thermo Fisher 26140-079) and kept on ice. Collected cells were centrifuged, filtered using 100 μ m cell strainer and resuspended in culture medium consisting of DMEM (Biochrom F0415), heat inactivated 10% Fetal Calf Serum (Thermo Fisher 26140-079), 1% penicillin/streptomycin (Thermo Fisher 15140-122), and 1% L-Glutamine (200 mM Gibco).

Generation of fibrin-based rEHTs

To generate fibrin-based rEHTs a reconstitution mixture was prepared on ice as follows: (final concentration): 6×10^6 cells/rEHT, 5 mg/mL bovine fibrinogen (Sigma F8630), DMEM $2 \times$ (20% DMEM $10 \times$, 20% heat inactivated horse serum [Thermo Fisher 26050-088], 1% penicillin/streptomycin [Thermo Fisher 15140-122]). Casting molds were prepared by adding 1.5 mL 2% agarose in PBS (Invitrogen 15510-027) per well in 24-well culture dishes and placing Teflon spacers inside. After agarose jellification, the spacers were removed ($L \times W \times D$ 12 mm \times 3 mm \times 4 mm) and silicone post racks were placed onto the dishes with pairs of posts reaching into each casting mould. For each rEHT 100 μ L reconstitution mix was mixed briefly with 3 μ L thrombin (100 U/mL, Sigma Aldrich T7513) and pipetted into the agarose slot. For fibrinogen polymerization, the constructs were placed in a humidified cell culture incubator at 37°C, 7% CO₂ for 2 h. To ease removal of the constructs from agarose casting molds, cell culture medium (300 μ L) was then added in each well. Racks were transferred to new 24-well cell culture dishes. rEHTs were maintained in 37°C, 7% CO₂ humidified cell culture incubator. Media was changed on Mondays, Wednesdays, and Fridays. rEHT medium consisted of DMEM (Biochrom F0415), 10% horse serum (Thermo Fisher 26050-088), 1% penicillin/streptomycin (Thermo Fisher 15140-122), insulin (10 μ g/mL, Sigma-Aldrich I9278), and aprotinin (33 μ g/mL, Sigma Aldrich A1153). rEHTs were visually expected every day and are considered mature approximately 10 days after the development of coherent beating.

Immunofluorescent analysis

rEHTs were fixed with 4% paraformaldehyde for 24 h and paraffin embedded. Four-micrometer thick tissue sections were de-waxed and rehydrated and processed for immunofluorescence. Antigen retrieval was performed by boiling sections in 10 mM Tris base, 1 mM EDTA solution and 0.05% Tween 20 at pH 9.0 for 20 min and left at room temperature for 2 h. Sections were rinsed three times in water and permeabilized 20 min in 0.25% Triton X-100 in PBS. For BrdU detection, DNA denaturation was performed by incubating section for 15 min in 0.1% Trypsin with 0.05% CaCl₂, then in 2 M HCl for 30 min at room temperature and finally the reaction was stopped with 0.1 M of

NaBorate solution pH 7.8. For EdU detection, slices were processed using the Click-IT EdU 594 Imaging kit (Life Technologies) to reveal EdU incorporation, according to the manufacturer's instructions, and counterstained with Hoechst 33342 (Life Technologies). rEHT sections were stained overnight at 4°C with a combination of these antibody: anti-cardiac troponin I antibody (ab47003), anti-cardiac troponin T antibody (ab8295), anti-BrdU (ab6323), anti-phospho-Histone 3 (Ser10) antibody (06-570), anti-Ki67 antibody (ab15580), anti-vimentin (5741S), and anti-collagen I (ab34710).

Gene expression analysis

Total RNA was isolated using TRIzol (Invitrogen). Mechanical sample homogenization was achieved using "Lysing Matrix D" (MPBio), for two 30 s cycles (6500 speed units) using a MagNA Lyser (Roche). Between cycles, samples were chilled in ice, and after homogenization, samples were always kept on ice unless stated otherwise. Supernatant was separated from tissue debris and phenol/chloroform extraction was performed. DNase/RNase free water was used to resuspend pellet and stored at -80°C. RNA concentration and quality was evaluated using Nanodrop 1000 Spectrophotometer (Thermo Fisher Scientific) and agarose gel electrophoresis. Reverse transcription was performed using the High-Capacity cDNA Reverse Transcription kit (Applied Biosystems) using random primers. Diluted cDNAs were used for quantitative assessment of RNA expression of selected genes using a BioRad CFX96 Touch™ Real-Time PCR Detection System. Results were normalized by the expression of housekeeping genes. TaqMan (Applied Biosystem) system was used to quantify levels of gene expression using TaqMan probes listed in Table 1 and following manufacturer's instruction. For each experimental condition, at least three biological replicates and two technical replicates were used. Fold change between control and treated samples was identified with $2^{-\Delta\Delta CT}$ method.

Video optical recording and analysis

rEHTs contraction was recorded with an Andor Neo sCMOS camera integrated in Nikon eclipse T1 using a Plan UW $2 \times$ objective that can perform live imaging using a dedicated humidified incubator at 37°C, 7% CO₂. Recording was performed for 10 s at 100 frames per second. For stimulated contraction measurements, rEHTs were electrical stimulated as previously describe (Hansen et al.⁷) at 4 Hz using a Hugo Sachs Elektronik Stimulator c type 224.

Based on post geometry, elastic modulus of Sylgard 184 (2.6 kPa) and delta of post distance (post deflection) force was calculated according to a published equation.¹¹ For a post of radius R and length L , cast from material with a known elastic modulus (E), the moment of inertia (I) is

Table 1. TaqMan probes.

Name	Gene	TaqMan code
Alpha smooth muscle actin	Acta2	Rn01759928_g1
Alpha-actinin-1	Actn1	Rn00667357_m1
Chemokine (C-C motif) ligand 2	CCL2	Rn00580555_m1
Collagen type I	Coll1a1	Rn01463848_m1
Fibronectin	Fn1	Rn00569575_m1
Interleukin 1 beta	Il1-β	Rn00580432_m1
Matrix metalloproteinase-12	Mmp12	Rn00588640_m1
Matrix metalloproteinase-2	Mmp2	Rn01538170_m1
TIMP metalloproteinase inhibitor 1	Timp1	Rn01430873_g1
Glyceraldehyde 3-phosphate dehydrogenase	GAPDH	Rn01775763_g1

given by $I = 1/4R^4$ and force based on post deflection δ by the formula:

$$F = \frac{3EI\delta}{L^3} = \frac{3\pi ER^4\delta}{4L^3} = \mu N$$

Cryoinjury

We built a custom-made system to deliver cryoinjury to the middle section of rEHTs. Briefly, a 50 mL tube was connected through a copper pipe to a 23 or 26 G needle that was bent to facilitate the contact with the rEHTs in a discrete fashion. The tube was filled with liquid nitrogen and the lid was used to direct the flow through the needle, thus creating a cryo-probe. The rEHT was placed in contact with the needle, while the liquid nitrogen was flowing, for 1 or 4 s and a clear area of freezing could be observed. The removal of the plunger would determine a stop of the flow through the needle and a rise in temperature that allows to safely detach the rEHT. After the procedure, rEHTs were placed in complete medium to recover.

Statistical analysis

All the results are expressed as mean \pm standard deviation (SD) or standard error of the mean (SEM). Student's *T*-test, one-way ANOVA, or two-way ANOVA tests were calculated using GraphPad Prism 6 (GraphPad Software, La Jolla California USA). Student's *T*-test was used to compare two groups, one-way ANOVA followed by Bonferroni's multiple comparison was used to compare multiple sample groups with one control, two-way ANOVA was used to compare multiple measurements of distinct sample groups. Statistical significance against control treatment was highlighted with "*" symbols as listed in the table below.

Animal ethics statement

Animal use was approved by the Italian Ministry of Health (reference number D441B.N.80Q). All animal procedures

Statistical significance	Symbol
$p > 0.05$	None
$p \leq 0.05$	*
$p \leq 0.01$	**
$p \leq 0.001$	***

performed conform to the guidelines from Directive 2010/63/EU of the European Parliament on the protection of animals used for scientific purposes.

Results

Cryoinjury discontinues the functional syncytium in rEHTs leading to significant, permanent loss of force of contraction

Among the available tissue models to investigate in vitro the cellular and molecular response to injury, hiPSC-derived CMs assembled in engineered cardiac tissues retain a proliferative potential that contributes to cardiac repair after injury, at least partially restoring the force of contraction;⁶ however, it is not clear whether the same can be observed in engineered tissues made from neonatal CMs, that develop a higher grade of maturation. To investigate this hypothesis, we developed a custom-made system to perform cryoinjury damage to the middle section of rEHTs (Figure 1): we connected a 50 mL Falcon tube filled with liquid nitrogen to a bent 23 G needle, in order to precisely damage with this cryo-probe the contractile EHT tissue in a discrete and reproducible fashion. Actually, the rEHT is placed in contact with the needle while the liquid nitrogen is flowing for 4 s, and a clear area of freezing can be observed. Then, the flow through the needle is stopped, the temperature rises, allowing to safely detach the rEHT from the cryo-probe in about 5 s. Subsequently, rEHTs were placed in complete medium to recover.

As previously described, after maturation (that occurs around day 10 post casting), rEHTs start beating as a functional syncytium and rhythmically deflect the silicone posts they are assembled in between.⁷ After cryoinjury, a significant loss of coherent beating in the whole rEHT was observed, characterized by two distinct areas next to each silicone post with independent contractile activity (Figure 1(b) and (c)), that however may be synchronized with electrical pacing.

Mature rEHTs were subjected to cryoinjury or sham injury ($n = 8$ per group) and the force of contraction was evaluated at different timepoints. rEHTs were video recorded at baseline, 24 h, and every 3 days after injury until day 11 (Figure 1(d) and (e)). After cryoinjury, the overall force of contraction was reduced by 50% and there was no recovery of contractile activity, suggesting that cardiac repair, if present, was not sufficient in our model to

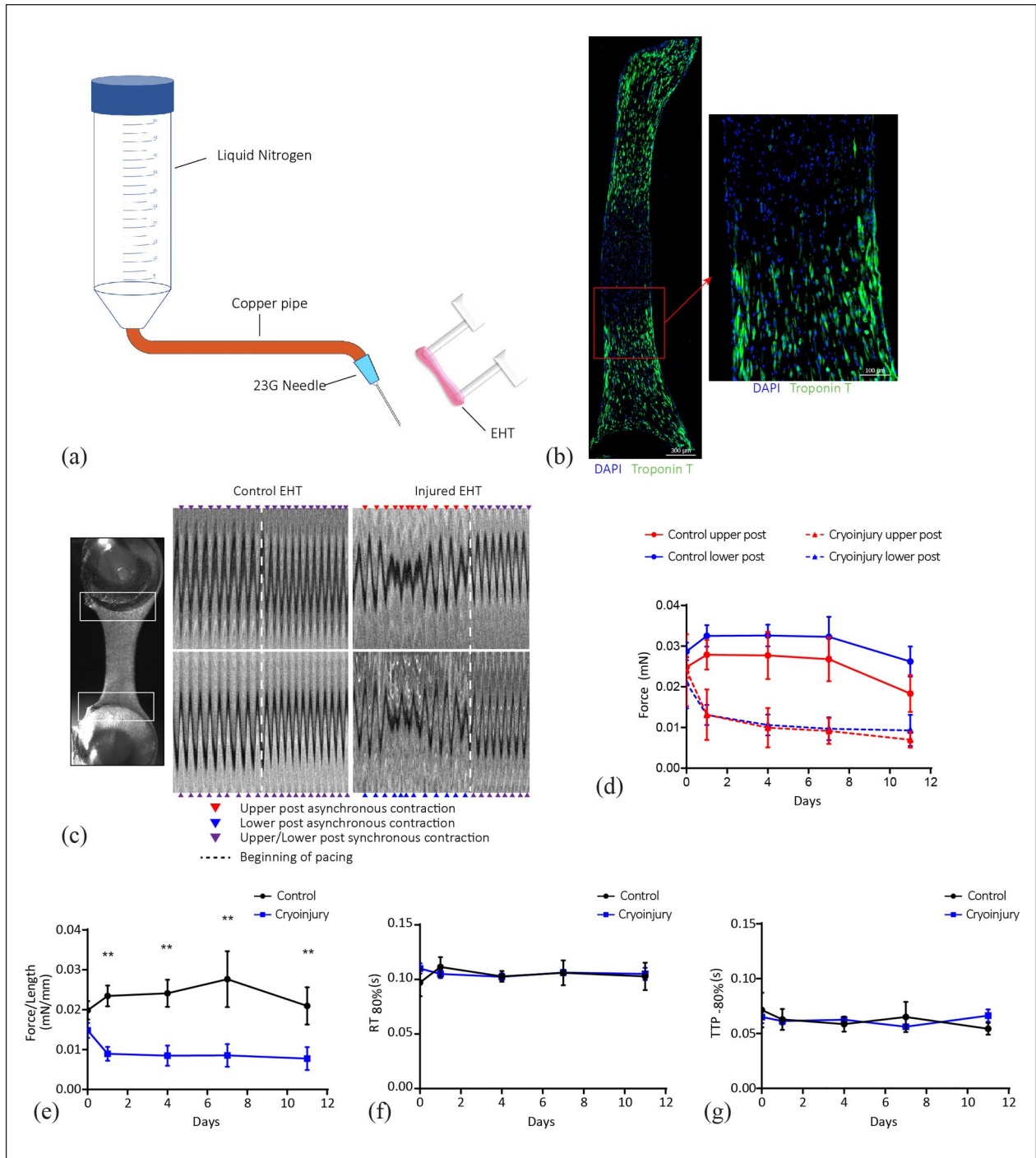


Figure 1. Cryoinjury induces a permanent loss of force of contraction in rEHTs: (a) schematic representation of the cryoinjury apparatus, (b) representative images with merged immunofluorescence staining for nuclei (blue) and troponin T (green) of rEHTs (scale bar: 300 μ m), (c) space-time representation (Kymograph) of rEHT contraction of the top post border and the bottom post border with and without pacing, (d) quantification of force of contraction exerted by the single posts in control and injured EHTs, (e) overall force of contraction does not recover in injured rEHTs over time, (f and g) Relaxation time (RT_{80%}) and time to peak (TTP_{80%}) do not change after cryoinjury. (Data shown as mean \pm SD).

restore the force of contraction, similar to what happens after injury to the adult mammalian cardiac tissue. Conversely, no significant difference was observed for time to peak (TTP_{80%}) and relaxation time (RT_{80%})

between cryoinjured and control EHTs over time (Figure 1(f) and (g)). These two functional parameters are largely force-independent and are reduced in pathological remodeling,¹² suggesting that the tissue response to cryoinjury

was not inducing, at least in the timeframe observed, structural and contractile changes.

Cryoinjury-induced DNA synthesis in mature EHT CMs does not translate into an increase of proliferation

Cryoinjury has been shown to induce an important CM proliferative response with tissue regeneration in human cardiac organoids.⁶ These and other recent evidences arose from human iPSC derived CMs, notoriously showing an “immature,” “fetal-like” phenotype,¹³ thus unsuitable to understanding the mechanism behind the lack of cardiac regeneration after MI in adults.

To test the hypothesis that “mature” rEHTs can at least in part recapitulate the adaptive response of adult myocardium to injury, we generated rEHTs as previously described and, following cryoinjury, we pulsed them with EdU at different time points (2, 4, 6, 8, and 10 days after cryoinjury). We observed a significant increase of EdU+CMs at day 6 and day 8 post injury, compared to baseline ($2 \pm 0.6\%$ vs $4.8 \pm 0.9\%$ vs 4.3 ± 1.6 ; Figure 2(a)). We also evaluated if DNA synthesis resulted in CM progression into the cell cycle. Comparing the number of CM scoring positive for Ki67 and pH3(Ser10), markers respectively of generic proliferation and mitosis, we could not detect any significant difference at the different timepoints after injury, suggesting that cryoinjury induces DNA synthesis but not CM mitosis in mature rEHTs. Recent evidence has shown that the lack of the proliferative response of CMs after MI is associated to DNA synthesis in CMs in the border-zone of the injured myocardium, leading to cell polyploidy and multinucleation, but not cell division.¹⁴ As shown in Figure 2(f) and (g), the number of binucleated CMs is not significantly different between injured EHTs and age-matched control at day 10 after cryoinjury (no multinucleated CMs were detected besides binucleated ones) thus we speculate that CM DNA synthesis may lead to polyploidy as shown in rodents after MI.¹⁴ Our data suggest that the cryoinjury model well parallels the biological response to injury of CMs in the adult heart and may represent a novel tool to investigate CM proliferation and biology in vitro.

Cryoinjury induces focal collagen deposition, decreasing over time

Cardiac fibroblasts are the most abundant cell type present in rEHTs, besides CMs.¹² It is known that fibroblasts have a pivotal role in modulating cardiac tissue response and outcome after MI, driving the formation of the fibrotic scar, by a sustained deposition of extracellular matrix (ECM), mostly of collagen I. Fibroblasts are activated by molecules released by dying CMs, in order to let them proliferate and promote the deposition of ECM, thanks to released anti-inflammatory and pro-fibrotic mediators.¹⁵

In order to further characterize the cellular and biochemical response of rEHTs after cryoinjury, focusing our interest on ECM features, we subjected mature rEHTs to cryoinjury and immunofluorescence analysis for collagen I was performed on tissues, harvested at different timepoints (baseline, day 2, day 4, and day 6 after injury). Quantification of areas that scored positive for collagen I show that collagen deposition shows a bell-shaped increase after injury, reaching a significant peak 4 days after injury (0.9 ± 0.4 vs $0.3 \pm 0.2\%$; Figure 3(a)) and lowering to the pre-injury levels at day 6. Moreover, as shown in Figure 3(b), we noticed that collagen-rich areas were not homogeneously distributed in the tissue, and independently from the site of the injury. We confirmed by immunofluorescence analysis the presence of vimentin positive fibroblasts inside the areas of collagen accumulation (Figure 3(e)). Gene expression analysis showed increased fibronectin (Fn1) and Collagen type 1 (Col1a1) mRNA levels in the early stage after cryoinjury as it has been shown in vivo after MI¹⁶ (Figure 3(c) and (d)).

Cryoinjury induces activation of fibroblasts localized at the injury border zone

Besides collagen deposition, another hallmark of an activated cardiac fibroblast is proliferation. Fibroblasts in the borderzone of the infarct increase in number and undergo to myofibroblast conversion, promoting the formation of a mature scar.¹⁷ To evaluate whether cryoinjury stimulates proliferation of rEHT resident fibroblasts, the number of EdU⁺ fibroblasts at different timepoints after injury was evaluated. rEHTs were generated as previously described and EdU was added to the medium every 48 h. Four rEHTs per timepoint were fixed at the baseline and at day 2, 4, 6, 8, and 10 after injury and the levels of EdU incorporation were compared to the uninjured control. Immunofluorescence staining for EdU revealed a progressive increase of DNA synthesis in Vimentin⁺ cells during the days following the injury (from 5.4% in the basal condition to 29.8% and 26.7% at day 2 and 4, respectively—Figure 4(a)). In the following timepoints, the number of EdU⁺ fibroblasts was comparable to the basal levels, suggesting that the contribution of cryoinjury to cell division is prevalent in the first 96 h after injury and is followed by a physiological turnover of non-CMs cells in rEHTs (Figure 4(a)). This observation was confirmed by the quantification of Ki67⁺TnT⁻ cells that show a similar trend after cryoinjury and by the significant increase of the number of Vimentin⁺ cells over the total number of TnT⁺ cells in the subsequent days (Supplemental Figure S1). Finally, as shown in Figure 4(c), the vast majority of EdU⁺ fibroblasts are localized at the borderzone, with a gradient lowering toward the remote area, suggesting that this pro-proliferative cue may be due to paracrine factors derived from

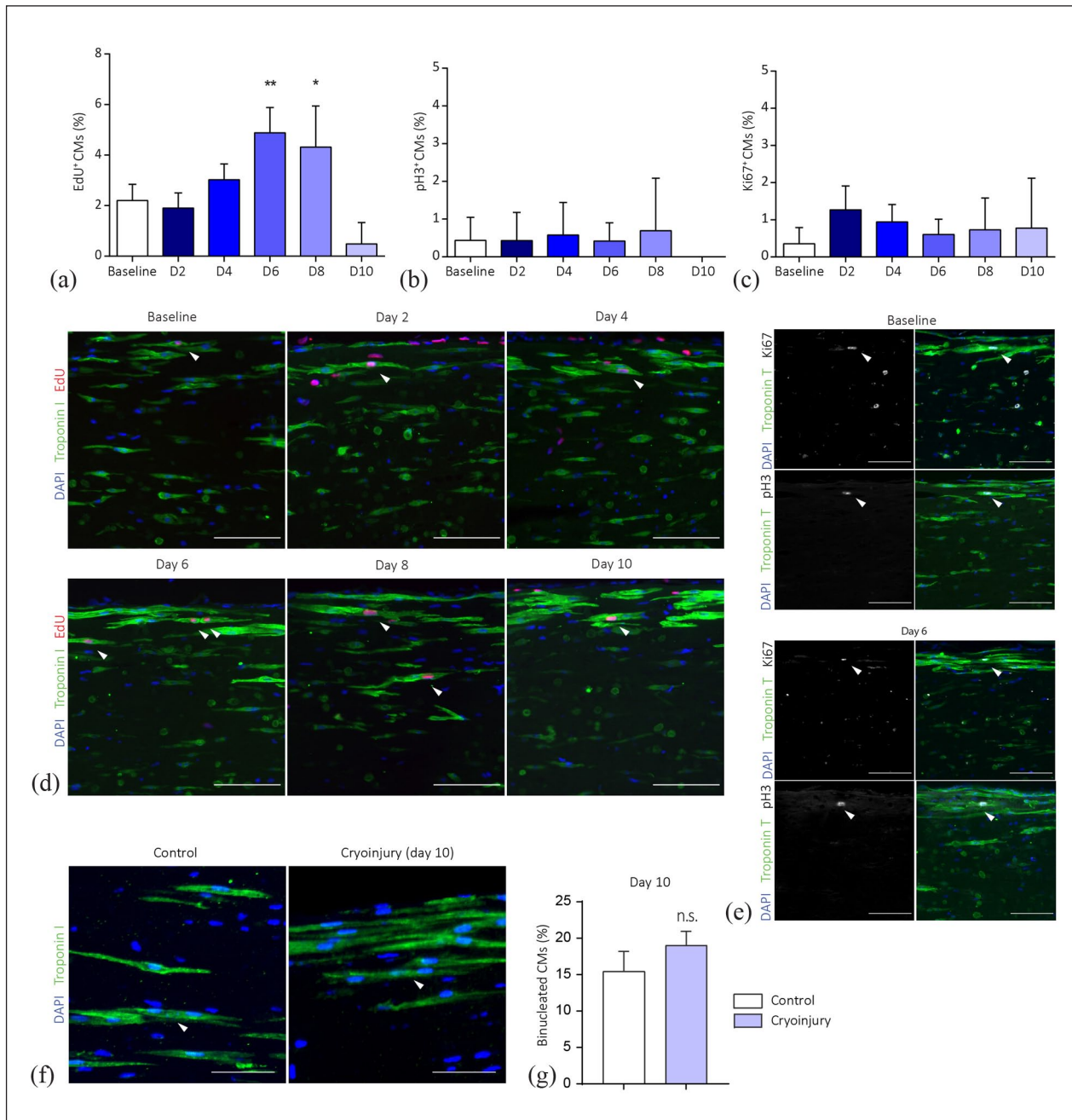


Figure 2. Cryoinjury induces CM DNA synthesis without cell division: (a–c) quantification of EdU⁺, Ki67⁺, and pH3⁺ CMs in rEHTs 2, 4, 6, 8, and 10 days after cryoinjury ($n=4$ per group). EdU was supplemented to the medium for a pulse of 48 h, every timepoint represents the proliferative window of the previous 2 days (data shown as mean \pm SD), (d and e) representative images with merged immunofluorescence staining for nuclei (blue), troponin I (green), EdU (red), and pH3 (white) of rEHTs (scale bar: 100 μ m). EdU⁺ CMs are highlighted with white arrows and pH3⁺ CMs with white stars, (f) representative images with merged immunofluorescence staining for nuclei (blue) and troponin I (green) of rEHTs at day 10 after cryoinjury (scale bar: 50 μ m), and (g) relative quantification. EdU⁺, pH3⁺, Ki67⁺, and binucleated CMs are highlighted with white arrows.

the injured part of the tissue. Their identification is ongoing.

To further investigate whether our model of cryoinjury may recapitulate in vivo fibroblast response to MI, gene expression analysis was performed measuring mRNA

levels of the pivotal genes involved in this process. In vivo, after MI, cardiac fibroblasts secrete cytokines and chemokines such as IL-1 and CCL2 to recruit and activate leukocytes^{18,19} and trigger the chemical activation of the injured area, characterized by the secretion of matrix

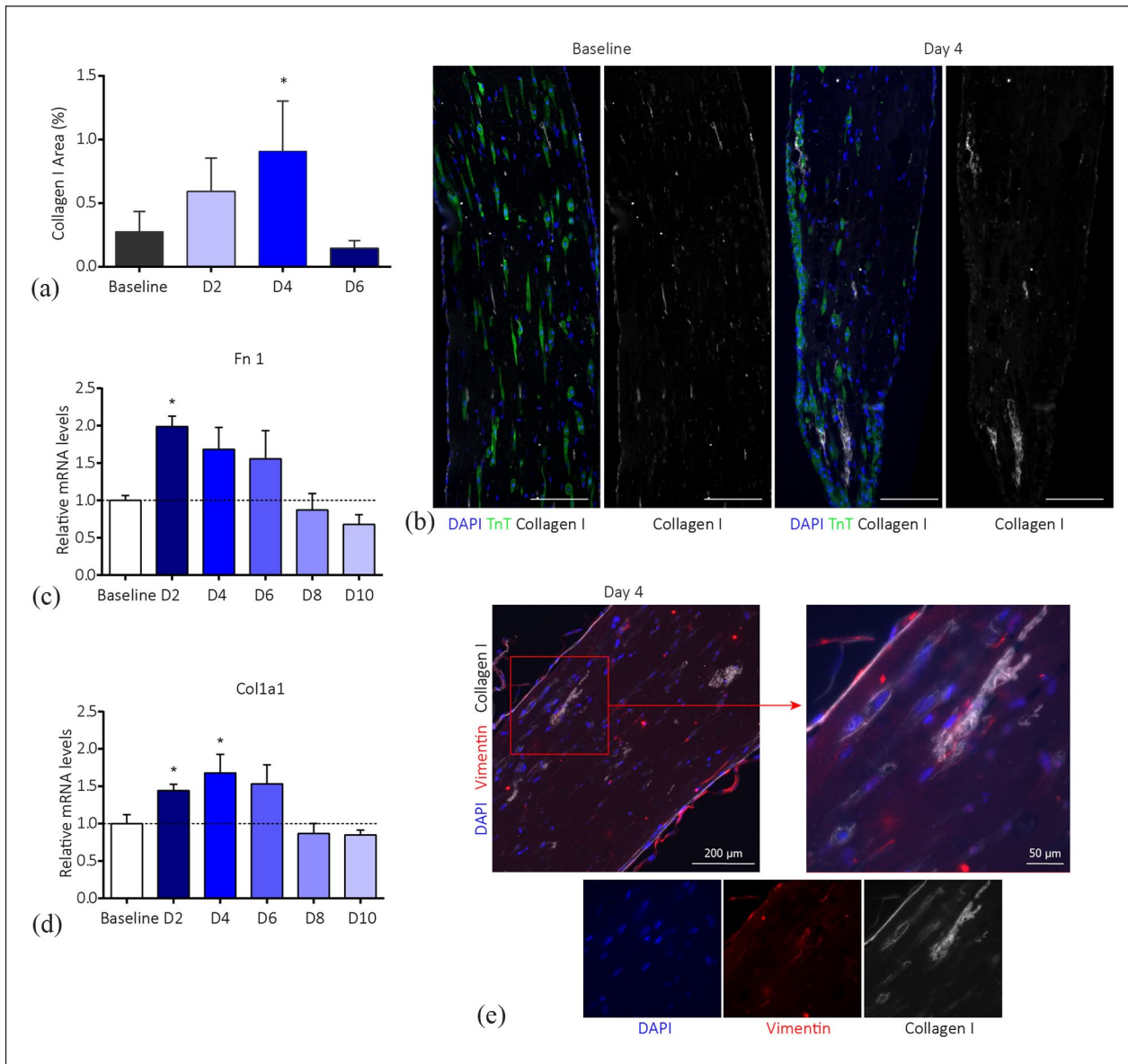


Figure 3. Cryoinjury induces focal collagen deposition in rEHTs: (a) quantification of Collagen I area over total area (data shown as mean \pm SD), (b) representative images of immunofluorescence staining for Collagen I (white) and images with merged immunofluorescence staining for nuclei (blue), troponin I (green) and Collagen I (white; Scale bar: 300 μ m), (c and d) relative mRNA levels of Fibronectin (Fn1) and Collagen I (Col1a1) over GAPDH in rEHTs at different timepoints after cryoinjury. ($n=4$ per group). (Data shown as mean \pm SEM), (e) on the left, representative image of a collagen accumulation (white) characterized by the presence of vimentin positive fibroblasts (red; scale bar:300 μ m). Higher magnification on the right (scale bar:100 μ m).

metalloproteinases (MMPs), promoting extracellular matrix degradation and release of pro-inflammatory matrix fragments.²⁰ In rats, MMP2 and MMP12 are two of the most relevant metalloproteinases involved in this process.^{5,21} To modulate the process and initiate an autoregulatory feedback loop, following the tissue activation, fibroblasts express inhibitors of metalloproteinases, such as Timp1, migrate to the MI borderzone, proliferate and undergo myofibroblast differentiation, incorporating alpha-SMA into cytoskeletal stress fibers.¹⁵ Mature rEHTs were

subjected to cryoinjury, harvested every 48 h ($N=4$ per group), and gene expression analysis was performed by RT-PCR. As shown in Figure 4(d), 48 h after injury, we observed a sudden and significant increase of pro-inflammatory molecules like CCL2 and IL-1 β ((3.9- and 2.3-fold change, respectively, when compared to uninjured controls), suggesting that damage-associated molecular patterns (DAMPs) deriving from dying cells stimulated fibroblasts to secrete cytokines and chemokines. Interestingly, CCL2 mRNA levels decreased over time,

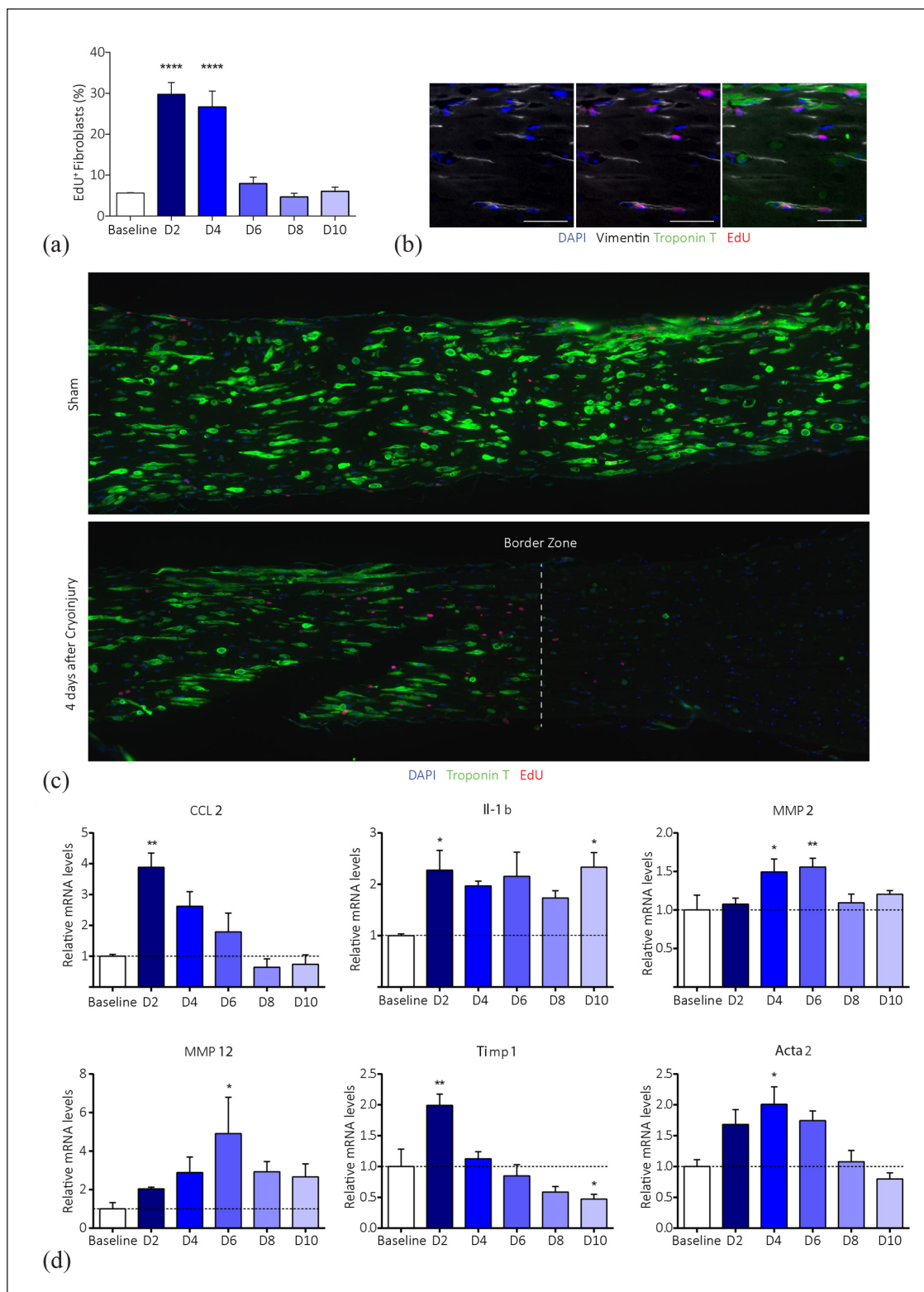


Figure 4. Cryoinjury induces fibroblast proliferation and activation: (a) quantification of EdU⁺ Vimentin⁺ cells in rEHTs from 2 to 10 days after cryoinjury. EdU was supplemented in 48h pulses to the medium starting from the 2 days before the injury until day 10, (b) representative images of proliferative vimentin positive fibroblasts (white) at day 4 after injury (scale bar: 50 μ m), (c) representative images with merged immunofluorescence staining for nuclei (blue), troponin I (green), EdU (red), and pH3 (white) of control rEHT (top), and injured rEHT (bottom). Dashed line highlights the borderzone. (Data shown as mean \pm SD), and (d) relative mRNA levels of chemokine (C-C motif) ligand 2 (CCL2), interleukin 1 beta (IL-1 β) metalloproteinases 2 and 12 (MMP2 and MMP12), metalloproteinase inhibitor 1 (Timp1) and α -SMA (Acta2) in rEHTs at different timepoints after cryoinjury (data shown as mean \pm SEM).

returning to pre-injury levels at day 4, while IL-1 β mRNA levels remained stable for all the subsequent timepoints. MMP2 and MMP12, early markers of matrix remodeling in vivo, significantly increased at day 2–3 post injury and decreased to baseline levels afterward (Figure 4(d)), suggesting a specific gene expression program driving the cellular response and matrix remodeling after injury, parallel to what happens in vivo.

The proliferative asset of CM in rEHT is crucial for the proliferative response after cryoinjury

The proliferative potential of rodent CMs is retained during a brief post-natal window and can produce an almost complete restitutio ad integrum after myocardial injury.^{1,22} This ability is lost after a week of post-natal life and in adults in case of injury, the contractile tissue is substituted by a fibrotic scar.^{23,24}

In order to better understand whether our cryoinjury model was able to resemble the CM responses upon cardiac injury at different stages of CM maturation, we first characterized the maturation process of EHTs, generally lasting two weeks to be completed. We subjected them to a 48 h pulse of BrdU at different time points between casting and the end of the window frame of interest (28 days post-casting) to evaluate CM proliferation. As shown in Supplemental Figure S2A, we observed that after an initial increase in the percentage of BrdU⁺ CMs early after rEHT casting (18% of BrdU⁺ CM at day 6), DNA synthesis progressively decreased, becoming almost negligible at day 28 (2% of BrdU⁺ CM). Interestingly, the decrease of BrdU⁺ CMs was paralleled by a progressive increase of binucleation, which is absent until day 4 post casting, rising to almost 20% in the latest phase of maturation (days 26–28; Supplemental Figure S2A-B). During the early stages of rEHT maturation, CMs beat independently, due to the lack of a functional syncytium, thus the displacement of the silicone posts is not detectable. Approximately between days 8 and 10, CMs develop a functional syncytium leading to spontaneous and coherent beating of the whole rEHT. As expected, the contractile strength increases during tissue maturation, reaching a plateau around day 22 (Supplemental Figure S2A-B). Indeed, on day 8 the percentage of BrdU⁺ CMs is significantly higher compared to day 20 while for binucleated CMs we observed an opposite trend. Considering that the “in vivo-like” CM organization in rEHTs is reached when the functional syncytium is developed, we arbitrarily defined “Day 8” as the reference time point for the “immature phase”, while “Day 20” will be stating for a “mature phase”. Gene expression analysis of some known markers of cardiac maturation confirmed our observations: as shown in Figure 5(a) and (b), the ratio between α and β myosin heavy chain (myh6/myh7)²⁵ gene expression levels and levels of sarcoplasmic/endoplasmic reticulum Ca²⁺ ATPase 2 (SERCA2a)

are significantly lower in immature rEHTs compared to mature ones ($1.2 \pm 0.2\%$ vs $2.1 \pm 0.5\%$ and $1.2 \pm 0.2\%$ vs $2.1 \pm 0.5\%$).

Therefore, we performed cryoinjury in “immature” rEHT the day after the onset of coherent beating, when a functional syncytium has just formed and DNA synthesis in CMs reached its peak (Supplemental Figure S2A), and we cryoinjured mature EHTs as a control group. As before, EdU was administered as a pulse of 48 h at day 4. As shown in Figure 5(c) we observed a significant increase of EdU⁺ CMs in immature rEHTs when compared to their controls ($6.3 \pm 1.9\%$ vs $10.1 \pm 1.6\%$ and $2.1 \pm 1.3\%$ vs $6.02 \pm 1.5\%$ EdU⁺ CMs respectively for immature and mature rEHTs). As expected, the number of Ki67 and pH3 positive CMs was not significantly increased in mature rEHT after cryoinjury. Interestingly, CMs increased DNA synthesis after cryoinjury in immature rEHTs was associated to a significant increase of Ki67⁺ and pH3⁺ CMs ($1.1 \pm 0.3\%$ and $1.3 \pm 0.3\%$ vs $0.4 \pm 0.1\%$ and $0.3 \pm 0.3\%$ of their age-matched control (Figure 5(d) and (e)), indicating that the degree of CM maturation plays a crucial role in the proliferative response after cryoinjury. We did not observe a significant change in binucleated CMs after cryoinjury in immature EHTs suggesting that the activation of the mitotic players led to cytokinesis events (Figure 5(f)).

We also characterized fibroblast response to cryoinjury in immature EHTs at day 4 post injury. As shown in Figure S3A, a not significant trend of increase in collagen deposition was observed in injured EHTs compared to control confirmed by the expression of collagen-1 and fibronectin-1 genes (Supplemental Figure S3C-D). Conversely, we observed a significant increase of EdU⁺ fibroblasts upon cryoinjury compared to control ($21.5 \pm 2.4\%$ vs $32.5 \pm 1.7\%$; Supplemental Figure S3E-F), whereas no significant changes were observed in gene expression of early markers of fibroblast activation and ECM remodeling (Supplemental Figure S3G-K). Taken together, these results indicate that cryoinjury induces an incomplete fibrotic response in immature EHTs suggesting that the mature environment, represented by mature CMs with higher contractile activity, is important for a proper fibroblast activation.

Discussion

One of the major limitations in performing high-throughput studies to fully characterize at a molecular level cardiac regeneration is the lack of reliable in vitro tissue-like models reliably mimicking what happens in vivo, after injury.² Recently proposed in vitro models take advantage of human iPSC-derived CMs, which allow a higher translatability of the findings, despite the immature phenotype of cells, aspect that reduces the robustness of the findings focused on characterize cardiac regeneration after MI in the adult.^{6,26} Cryoinjury has shown to induce tissue

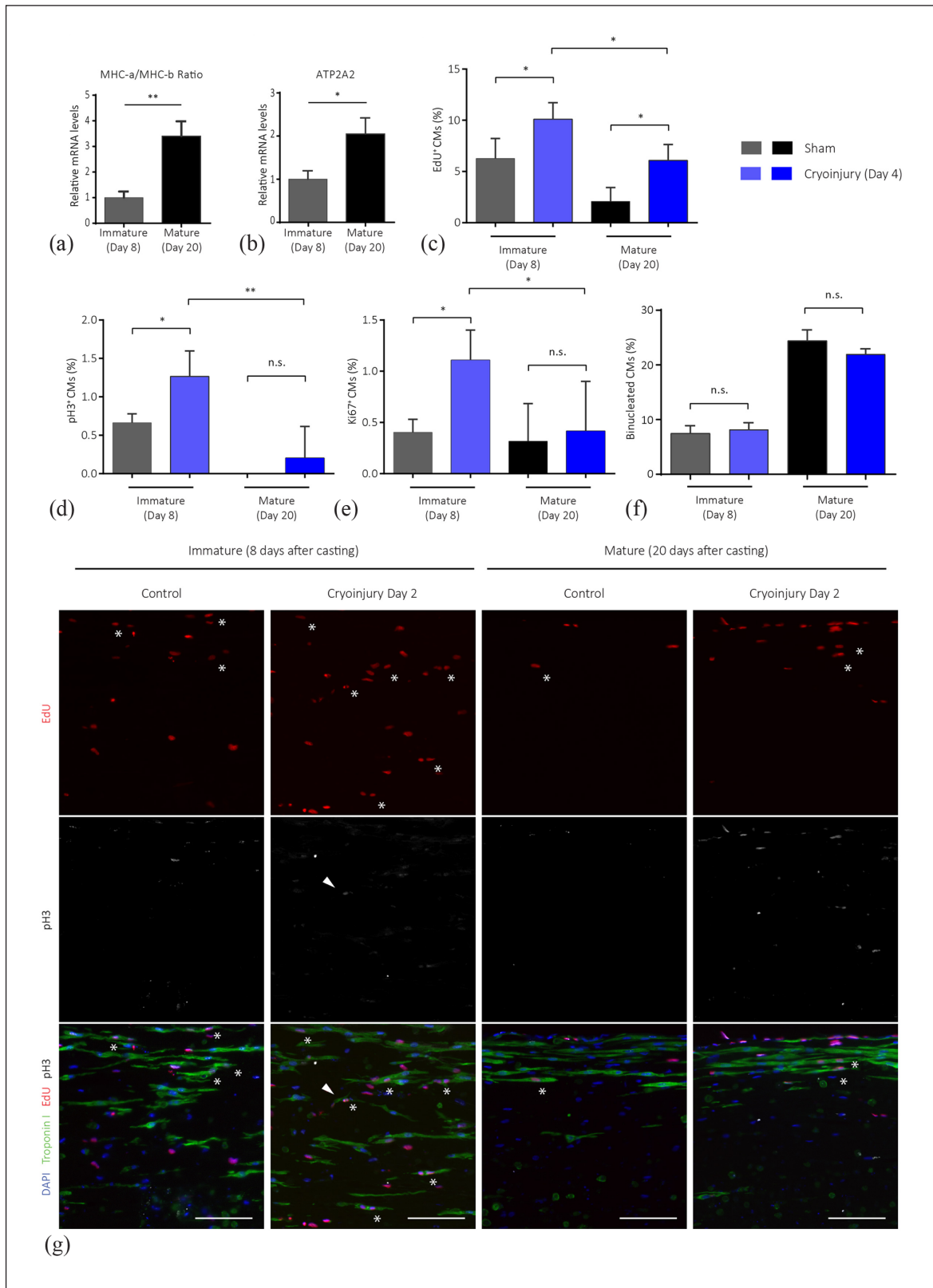


Figure 5. Cryoinjury induces CM proliferation in immature rEHTs: (a and b) relative mRNA levels of α - and β -myosin heavy chain and SRCa²⁺ ATPase 2 (SERCA2a) over GAPDH in rEHTs at day 8 and day 20. ($n=4$ per group). (Data shown as mean \pm SEM), (c–f) quantification of EdU⁺, Ki67⁺, pH3⁺, and binucleated CMs after 4 days from cryoinjury performed in immature (2 days after coherent beating that occurred at day 6) and mature rEHTs (18 days after casting; $n=4$ per group). EdU was supplemented to the medium for a pulse of 48 h (data shown as mean \pm SD), and (g) representative images with merged immunofluorescence staining for nuclei (blue), troponin I (green), EdU (red), and pH3 (white) of rEHTs (scale bar: 100 μ m). EdU⁺ CMs are highlighted with white arrows and pH3⁺ CMs with white stars.

regeneration in human cardiac organoids, which, however, show a robust proliferative response after injury typical of embryonic cells they are derived from, inevitably lost in adulthood. Conversely, rEHTs have the advantage of being an unpurified, native heart cell mix, which includes fibroblasts and endothelial cells, organized in an *in vivo*-like beating structure, recapitulating in part the tissue biology of the adult rodent heart, thus representing an exciting candidate to evaluate the response of myocardial injury at a molecular level. In our study, we used rEHTs as a model to characterize *in vitro* the cellular and molecular response to ischemic injury in an asset of adult rodent cells. *In vivo*, it has been shown that cryoinjury induces a necrotic wound of consistent size and shape that resolves into a scar of uniform size, shape, and organization, generating an extended injury border zone that exhibits classic markers of remodeling found in surviving animals.^{8,9} Thus, we set up a cryoinjury protocol with a custom-made system to deliver a discrete injury in rEHTs. Our system is feasible and reproducible, allowing to induce injuries of different sizes in localized areas of the engineered tissue. We established that cryoinjury produces a localized and reproducible injury in rEHTs, leading to a selective loss of contractile activity accompanied by electrical isolation.

We also tested the robustness of rEHTs as a model to investigate CM proliferation in EHT during the process of *in vitro* maturation. Similar to what has been shown in mice and rats early after birth,¹⁰ we demonstrated for the first time that in the rEHTs neonatal CMs preserve their proliferative capacity in the first week of tissue development, while the functional syncytium is not formed yet. As soon as CMs start to beat coherently, DNA synthesis progressively decreases in parallel to the increase of binucleation of CMs, resembling the switch from a neonatal to a more mature phenotype that occurs *in vivo*. A key concept in cardiac regenerative medicine is the strong correlation between regeneration and development. Wound healing of neonatal cardiac tissue after MI is characterized by an almost complete regeneration of the lost tissue, with barely detectable scar tissue. Conversely, adult cardiac tissue fails to regenerate CM loss after injury, resulting in scar formation.^{10,27} In a similar way, we demonstrate that cryoinjury induces DNA synthesis in CMs in immature rEHTs, while mature EHTs lack a proper proliferative response. Our results, therefore, strengthen rEHTs as a model mimicking *in vivo* post-natal CM maturation and cardiac regeneration upon injury in different stages of heart development. We also investigated the role of cardiac fibroblast in these settings. Cardiac fibroblasts are indeed one of the most abundant cell populations in rEHTs, besides CMs.¹² Fibroblasts have a pivotal role in tuning the cardiac tissue response and outcome after MI. One of the most important functions of fibroblasts is the formation of fibrotic tissue, characterized by a sustained secretion of ECM, mostly formed by collagen-I. Fibroblasts are activated by the ischemic event, mainly by molecules released by dead CMs, and are

induced to proliferate and undergo to maturation through anti-inflammatory and pro-fibrotic mediators to promote the deposition of ECM.¹⁵ In our study, we show that cryoinjury in rEHTs induces fibroblast temporary activation and proliferation, together with ECM deposition, overall mimicking only the early fibroblast cellular and molecular response occurring upon injury in the *in vivo* adult injured myocardium. The lack in our model of a persistent fibrotic response that in the injured myocardium produces a stable fibrotic scar may be related to the absence of the immune system, representing an important limitation that could be overcome by introducing cytokines and immune cells in the system. While we acknowledge that this represents a major limitation, we believe that the absence of the immune system contribution could facilitate the understanding of the cellular response of fibroblasts and CMs to injury. In conclusion, this is the first study that characterizes the regenerative response of rEHT after injury in the different phases of tissue maturation, when assembled cells are similar either similar to neonatal or adult CMs. Moreover, this system represents a robust and reproducible novel model to investigate some critical aspects of MI biology. Considering that the mechanism behind the discordant response to injury of neonatal and adult myocardium is still unclear, we argue that our model provides a unique opportunity to unravel the molecular and cellular mechanisms regulating the regenerative process. Indeed, the absence of a specific role driven by the inflammatory response upon injury and by the host immune system, major players in the cellular and molecular response after injury, may be seen as an advantage of rEHTs, in order to specifically dissect the peculiar role of either CM or fibroblasts after the ischemic damage.

Declaration of conflicting interests

The author(s) declared no potential conflicts of interest with respect to the research, authorship, and/or publication of this article.

Funding

The author(s) disclosed receipt of the following financial support for the research, authorship, and/or publication of this article: The authors would like to disclose and acknowledge the following financial support for the research and publication of this article from Programma V:ALERE 2019 Omics ACS, Fondazione CRTrieste, Fondazione CARIGO and Fincantieri S.p.A..

ORCID iD

Francesco S Loffredo  <https://orcid.org/0000-0001-5911-780X>

Data availability

The data underlying this article will be shared on reasonable request to the corresponding author.

Supplemental material

Supplemental material for this article is available online.

References

1. Porrello ER, Mahmoud AI, Simpson E, et al. Transient regenerative potential of the neonatal mouse heart. *Science* 2011; 331: 1078–1080.
2. Mills R and Hudson J. An in vitro model of myocardial infarction. *Nat Biomed Eng* 2020; 4: 366–367.
3. Pushp P, Nogueira DES, Rodrigues CAV, et al. A concise review on induced pluripotent stem cell-derived cardiomyocytes for personalized regenerative medicine. *Stem Cell Rev Rep* 2021; 17: 748–776.
4. Koivumaki JT, Naumenko N, Tuomainen T, et al. Structural immaturity of human iPSC-derived cardiomyocytes: In silico investigation of effects on function and disease modeling. *Front Physiol* 2018; 9: 80.
5. Ahmed RE, Anzai T, Chanthra N, et al. A brief review of current maturation methods for human induced pluripotent stem cells-derived cardiomyocytes. *Front Cell Dev Biol* 2020; 8: 178.
6. Voges HK, Mills RJ, Elliott DA, et al. Development of a human cardiac organoid injury model reveals innate regenerative potential. *Development* 2017; 144: 1118–1127.
7. Hansen A, Eder A, Bonstrup M, et al. Development of a drug screening platform based on engineered heart tissue. *Circ Res* 2010; 107: 35–44.
8. Polizzotti BD, Ganapathy B, Haubner BJ, et al. A cryoinjury model in neonatal mice for cardiac translational and regeneration research. *Nat Protoc* 2016; 11: 542–552.
9. Strungs EG, Ongstad EL, O’Quinn MP, et al. Cryoinjury models of the adult and neonatal mouse heart for studies of scarring and regeneration. *Methods Mol Biol* 2013; 1037: 343–353.
10. Lam NT and Sadek HA. Neonatal heart regeneration: comprehensive literature review. *Circulation* 2018; 138: 412–423.
11. Vandenburg H, Shansky J, Benesch-Lee F, et al. Drug-screening platform based on the contractility of tissue-engineered muscle. *Muscle Nerve* 2008; 37: 438–447. DOI: 10.1002/mus.20931
12. Hirt MN, Sorensen NA, Bartholdt LM, et al. Increased afterload induces pathological cardiac hypertrophy: a new in vitro model. *Basic Res Cardiol* 2012; 107: 307.
13. Guo Y and Pu WT. Cardiomyocyte maturation: new phase in development. *Circ Res* 2020; 126: 1086–1106.
14. Senyo SE, Steinhauser ML, Pizzimenti CL, et al. Mammalian heart renewal by pre-existing cardiomyocytes. *Nature* 2013; 493: 433–436.
15. Humeres C and Frangogiannis NG. Fibroblasts in the infarcted, remodeling, and failing heart. *JACC Basic Transl Sci* 2019; 4: 449–467.
16. Moore-Morris T, Cattaneo P, Guimaraes-Camboa N, et al. Infarct fibroblasts do not derive from bone marrow lineages. *Circ Res* 2018; 122: 583–590.
17. Weber KT, Sun Y, Bhattacharya SK, et al. Myofibroblast-mediated mechanisms of pathological remodeling of the heart. *Nat Rev Cardiol* 2013; 10: 15–26.
18. Bujak M, Dobaczewski M, Chatila K, et al. Interleukin-1 receptor type I signaling critically regulates infarct healing and cardiac remodeling. *Am J Pathol* 2008; 173: 57–67.
19. Dewald O, Zymek P, Winkelmann K, et al. CCL2/monocyte chemoattractant protein-1 regulates inflammatory responses critical to healing myocardial infarcts. *Circ Res* 2005; 96: 881–889.
20. Phatharajaree W, Phrommintikul A and Chattipakorn N. Matrix metalloproteinases and myocardial infarction. *Can J Cardiol* 2007; 23: 727–733.
21. Iyer RP, Patterson NL, Zouein FA, et al. Early matrix metalloproteinase-12 inhibition worsens post-myocardial infarction cardiac dysfunction by delaying inflammation resolution. *Int J Cardiol* 2015; 185: 198–208.
22. Porrello ER and Olson EN. A neonatal blueprint for cardiac regeneration. *Stem Cell Res* 2014; 13: 556–570.
23. Walsh S, Ponten A, Fleischmann BK, et al. Cardiomyocyte cell cycle control and growth estimation in vivo—an analysis based on cardiomyocyte nuclei. *Cardiovasc Res* 2010; 86: 365–373. 20100113.
24. Soonpaa MH, Koh GY, Klug MG, et al. Formation of nascent intercalated disks between grafted fetal cardiomyocytes and host myocardium. *Science* 1994; 264: 98–101.
25. McNally EM, Kraft R, Bravo-Zehnder M, et al. Full-length rat alpha and beta cardiac myosin heavy chain sequences. Comparisons suggest a molecular basis for functional differences. *J Mol Biol* 1989; 210: 665–671.
26. Hofbauer P, Jahnke SM, Papai N, et al. Cardioids reveal self-organizing principles of human cardiogenesis. *Cell* 2021; 184: 3299–3317.
27. Cardoso AC, Pereira AHM and Sadek HA. Mechanisms of neonatal heart regeneration. *Curr Cardiol Rep* 2020; 22: 33.